

The Impact of Jumps and Microstructure Noise on Forecasting Risk and Pricing Options*

Ai-ru (Meg) Cheng[†] Rituparna Sen[‡]

July 13, 2010

*The authors would like to thank Hans-Georg Müller for Matlab programs for FDA. The data was bought from the company 'Disktrading' and Olsen Financial Technologies 'OFT'.

[†]University of California at Santa Cruz, Department of Economics, 1156 High Street, Santa Cruz, CA 95064, USA. Phone: 831-459-2318. Email: airucheng@gmail.com.

[‡]University of California at Davis, Department of Statistics, 4218 Mathematical Sciences Building, One Shields Avenue, Davis, CA, 95616. USA. Phone: 530-564-0602. Email: rsen@wald.ucdavis.edu.

Abstract

The paper studies the contribution of jumps and microstructure noise in high frequency financial data to practical applications of forecasting risk, future volatility and option pricing. Tests of jump detection based on power variation, scale variation and functional data methods are considered. We carry out thorough simulation studies on the performance of the competing tests under different data generating processes and noise structures. Separating the total quadratic variation into components of smooth volatility, jump and microstructure noise, we examine the forecast accuracy of various components in the context of the realized volatility, Value at Risk, Expected shortfall and implied volatility.

Keywords: Volatility; high-frequency data; Expected Shortfall; functional data analysis; implied volatility; jumps; microstructure noise; realized variance; Value at Risk; Principal Component Analysis.

JEL Classification: C14, C22, G13.

1 Introduction

Over the past few decades, standard volatility models such as ARCH and GARCH (introduced by Engle (1982) and Bollerslev (1986)) and stochastic volatility (introduced by Clark (1973)) have been frequently used for estimating return volatility. However, this model-based approach casts a major concern because of its seemingly poor performance in volatility forecasts. The recent availability of databases recording intraday price movements has spurred a lot of activity in nonparametric approach for estimating the volatility. This model-free proxy for volatility, termed realized volatility, is grounded in the framework of continuous-time finance and is related to the notion of quadratic variation of a martingale. As introduced in Andersen et. al. (2003) and Barndorff-Nielsen and Shephard (2004), daily realized volatility is computed as the sum of the squared intraday returns. If prices follow a continuous path and are not contaminated by microstructure noise, Andersen, Bollerslev and Meddahi (2004) shows that simple time series models used to fit the realized volatility outperform the above mentioned model-based approaches for forecasting future volatility.

In modern financial economics, a continuous-time model is often used to describe price changes because of its analytical tractability. However, financial markets have long been noted to exhibit abnormally large price movements that are unable to be explained by a pure diffusive model. Hence, it is readily important to accommodate these unusual dynamics, referred to as jumps, when modeling a price change process. Due to, for example, extreme market events or macro announcements, price processes may present unusually large movements relative to what diffusive models would imply. In the framework of realized volatility, Andersen, Bollerslev and Diebold (2007) shows that many price processes are best described by separating the smooth persistent volatility component and much less persistent jump processes.

In order to detect jumps, many empirical literature has built upon the theoretical results in Barndorff-Nielsen and Shephard (2006) and Huang and Tauchen (2005) using variation measures constructed from the summation of scaled products of adjacent or staggered intraday absolute returns. The basic idea of the test is to construct a measure of variance, termed bipower variation, which is robust to the presence of jumps and subtract the measure from the total variance. A statistical significance of the difference, based on the asymptotic distribution of the test statistic, would indicate the occurrence of jumps. Their approach is powerful and appealing as it is model-free and straightforward to implement the tests. Ait-Sahalia and Jacod (2009) propose a test that is based on scale variation, that is, consider the ratio of volatility measures based on two different time scales. Among other jump detection methods, instead of using bipower variation, Jiang and Oomen (2008) uses cumulative hedged gain or loss based on a variance swap strategy. All the jump detection methods mentioned before are designed to indicate the presence and size of jumps during a certain interval; however, Lee and Mykland (2008) focuses on detecting the presence

of jump at any instantaneous time point in that interval.

Nowadays stock price and foreign exchange rate data are available at very high frequency. While more data implies more efficient estimation and prediction of daily volatility, it also means that the microstructure noise cannot be ignored any more. In a stochastic volatility model framework, Bandi and Russell (2006), Hansen and Lunde (2006), Oomen (2005) and Zhang, Mykland and Ait-Sahalia (2005) develop schemes to correct the bias due to the noise by calculating the realized volatility by optimal or mixing sampling scales. Barndorff-Nielsen et. al. (2009) do this using realized kernels and Jacod et. al. (2009) apply a pre-averaging method. As the problem of microstructure noise arises in the realized volatility calculated using high frequency data, results inferred from the above mentioned jump detection tests become subject to bias.

Müller, Sen and Stadtmüller (2007) introduce Functional Data Analysis (FDA) as a novel tool for modeling daily volatility trajectories. The FDA method borrows strength from data on all days to estimate the volatility pattern of one day by looking for common patterns in volatility trajectories, in contrast with existing non-parametric smoothing techniques like kernels or wavelets (Fan and Wang (2007)). Sen (2009) develops a method to simultaneously separate the smooth volatility, jump and market microstructure noise components of the total realized variance.

In this paper, we use the jump test statistic based on this decomposition. We examine the empirical rejection rate of this test statistic in comparison with other jump tests based on the power variation and scale variation via simulation. We study robustness of different methods with respect to different models and error distributions. Our empirical analysis focuses on studying the predictive power of the return quantiles (VaR) computed across different measures of the realized volatility using exchange rate data. We compare the accuracy of one-step-ahead VaR forecasts by modeling the smooth components of realized volatility following different test procedures. In a similar area of interest, we compare the accuracy of forecasts on the Expected Shortfall (ES) with the realized variance measures concluded by various jump detection methods. Also, in light of Andersen, Bollerslev and Diebold (2007) and Lanne (2007), we study whether different separation methods would matter in forecasting realized variance. Finally, we examine the forecasting power of the at-the-money implied volatility (IV) for the future volatility integrated over the life of the option based on different variation measures.

The contribution of the paper is to provide a link between jump detection in high frequency data and practical concerns of risk forecasting and option pricing. Although there has been some work on using high frequency data for VaR estimation, to our knowledge, these do not include a study of how the jump and microstructure noise can affect this estimation. We study the relative performance of various estimators of volatility from high frequency data in practical applications using simulations and real observations.

The rest of the paper is organized as follows. In section 2, we briefly review various jump test methods existing in the literature. In particular we present a brief review of functional data analysis and outline how we apply this technique to separate out the volatility from microstructure noise. In section 3, we launch a simulation study to show how ignoring noise leads to unrealistic test results in detecting jumps. In section 4, we describe the data for our empirical study. In section 5 and 6, we study the VaR forecasts of the return distribution using various realized variation measures. In section 7, we study relative performance of using different jump detection methods in forecasting realized volatility. In section 8, we revisit the relationship between the implied volatility and future integrated volatility. Specifically, we look at the role of each variation method plays in explaining the gap between the implied volatility and integrated realized volatility. Finally in section 9, we present our conclusions.

2 Jump Detection and Decomposition of the realized variance

In this section, we describe the methods of jump detection, namely bipower variation referred to as BNS, staggering referred to as HT, scale variation and functional data analysis referred to as FDA. We present the decomposition of the daily realized variance using the FDA method into three components : smooth volatility, jumps and the variation due to the noise.

2.1 Jump Detection using Bipower variation

Let $p_t = \log(P_t)$ denote the logarithmic price of the asset at time t . We assume that P_t follows the jump diffusion process:

$$dp_t = \mu_t dt + \sigma_t dW_t + J_t dq_t \quad (1)$$

where μ_t and σ_t are the drift and diffusion functions that are subject to the mild regularity conditions in Muller, Sen and Stadtmuller (2007), W_t is the standard Brownian motion, q_t is a Poisson process with intensity λ , and J_t denotes the jump size.

We are interested in the time interval $(t-1, t)$. Suppose the price process is observed at times $t-1 \leq t_1 \leq \dots \leq t_j \leq t$ which are at time interval Δ apart within each day. Let y_{t_j} be the log returns at time t_j

$$y_{t_j} = p_t(t_j) - p_t(t_{j-1}) \quad (2)$$

Barndorff-Nielsen and Shephard (2004) proposes using realized variance to ap-

proximate the daily quadratic variation process

$$RV_t = \sum_{j=1}^{[1/\Delta]} y_{t_j}^2 \xrightarrow[\text{as } \Delta \rightarrow 0]{P} \int_{t-1}^t \sigma_s^2 ds + \int_{t-1}^t J_s^2 d[q]_s \quad (3)$$

and derives a bipower variation method based on the adjacent returns for the continuous component of the variance process:

$$BNS_t = \frac{\pi}{2} \left(\frac{[1/\Delta]}{[1/\Delta] - 1} \right) \sum_{j=2}^{[1/\Delta]} |y_{t_{j-1}}| |y_{t_j}| \xrightarrow[\text{as } \Delta \rightarrow 0]{P} \int_{t-1}^t \sigma_s^2 ds \quad (4)$$

Following the bipower variation in equation (4), one can inspect for days with abnormal price movements according to the asymptotic result of the ratio statistics (termed BNS test statistics):

$$z_{BNS,t} = \frac{RV_t - BNS_t}{\sqrt{((\frac{\pi}{2})^2 + \pi - 5) \frac{1}{[1/\Delta]} TP_{BNS,t}}} \xrightarrow[\text{as } \Delta \rightarrow 0]{d} \mathbf{N}(0, 1) \quad (5)$$

where $TP_{BNS,t}$ is denoted as the tri-power variation

$$TP_{BNS,t} = \mu_{4/3}^{-3} \frac{[1/\Delta]}{[1/\Delta] - 2} \sum_{j=3}^{[1/\Delta]} |y_{t_{j-2}}|^{4/3} |y_{t_{j-1}}|^{4/3} |y_{t_j}|^{4/3} \quad (6)$$

$$\mu_k = 2^{k/2} \Gamma[(k+1)/2] / \Gamma(1/2) \quad (7)$$

2.2 Jump detection in the presence of microstructure noise using Staggering

Due to several frictions in the market like the bid-ask spread, recording errors, discreteness of prices etc., prices may be observed differently from the true process. The existence of these practical findings, termed as microstructure noise, complicates the use of high-frequency data for calculating RV as well as volatility components. Since Zhou (1996), the notion of how to correct the bias in RV contaminated by the cumulative microstructure noise has been discussed extensively in Bandi and Russell (2006), Ait-Sahalia, Mykland and Zhang (2005), Hansen and Lunde (2006), Zhang, Mykland and Ait-Sahalia (2005), and many others. Huang and Tauchen (2005) conducts a thorough simulation study on the bipower variation separation method and finds that the test is biased downward in detecting jumps as the sampling frequency increases. Given the presence of microstructure noise and some regular assumptions for the noise distribution, Huang and Tauchen (2005) provides a theoretical justification for the bias in BNS test and suggests to correct the bias by staggering the absolute returns in bipower and tri-power variation (4) and (6):

$$HT_t = \frac{\pi}{2} \left(\frac{[1/\Delta]}{[1/\Delta] - 1} \right) \sum_{j=3}^{[1/\Delta]} |y_{t_{j-2}}| |y_{t_j}| \xrightarrow[\text{as } \Delta \rightarrow 0]{P} \int_{t-1}^t \sigma_s^2 ds \quad (8)$$

$$TP_{HT,t} = \mu_{4/3}^{-3} \frac{[1/\Delta]}{[1/\Delta] - 4} \sum_{j=5}^{[1/\Delta]} |y_{t_{j-4}}|^{4/3} |y_{t_{j-2}}|^{4/3} |y_{t_j}|^{4/3} \quad (9)$$

$$\mu_k = 2^{k/2} \Gamma[(k+1)/2] / \Gamma(1/2) \quad (10)$$

$$z_{HT,t} = \frac{RV_t - HT_t}{\sqrt{((\frac{\pi}{2})^2 + \pi - 5) \frac{1}{[1/\Delta]} TP_{HT,t}}} \xrightarrow[\text{as } \Delta \rightarrow 0]{d} \mathbf{N}(0, 1). \quad (11)$$

Although HT is expected to detect more jumps than those BNS would imply, it may, however, introduce an upward bias when it is used to detect jumps.

2.3 Jump detection using scale variation: AS-J method

Aït-Sahalia and Jacod (2009) have recently proposed an alternative jump detection method. Under the null hypothesis of no jumps and in the absence of microstructure noise, the test statistics of z_{AS-J} converges to a standard normal random variable¹

$$z_{AS-J,t} = \hat{V}_c^{-1/2} \left(\frac{\hat{B}(\gamma, k)_t}{\hat{B}(\gamma, 1)_t} - k^{\gamma/2-1} \right), \quad \gamma \geq 2 \quad (12)$$

Where

$$\begin{aligned} \hat{B}(\gamma, k) &= \sum_{j=1}^{[1/(k\Delta)]} |p_t(t_{kj+1}) - p_t(t_{k(j-1)+1})|^\gamma \\ \hat{V}_c &= \frac{\Delta M(\gamma, k) \hat{A}(2\gamma, \Delta)_t}{\hat{A}(\gamma, \Delta)_t^2} \\ \hat{A}(\gamma, \Delta) &= \frac{\Delta}{m_\gamma} \sum_{j=1}^{[1/\Delta]} |p_t(t_j) - p_t(t_{j-1})|^\gamma \mathbf{1}_{|p_t(t_j) - p_t(t_{j-1})| \leq a\Delta^b}, \quad a > 0, b \in \left(0, \frac{1}{2}\right) \end{aligned}$$

where $M(\gamma, k)$, m_γ and $m_{k,\gamma}$ are nonrandom functions defined in Aït-Sahalia and Jacod (2009); parameter a is advised to be selected as 3 to 5 times the long-run mean of the volatilities; parameter b is chosen to be close to 0.5 as detailed in Aït-Sahalia and Jacod (2009).

¹See details in Aït-Sahalia and Jacod (2009).

The intuition for the behavior of the test statistic $z_{AS-J,t}$ is that when $\gamma > 2$ the term $\hat{B}(\gamma, 1)$ in equation (12), the numerator $\hat{B}(\gamma, k)$ is expected to be more dominated by the large jumps in prices with $k > 1$, as its summands are constructed by the difference of two prices that are further apart from each other.

2.4 Jump detection using FDA method

Müller, Sen and Stadtmüller (2007) introduces a method of functional volatility process as a tool for modeling and estimating volatility. They consider the volatility trajectory of each day to be a realization from the distribution of smooth volatility processes in combination with a multiplicative noise. Although Todorov and Tauchen (2010) suggests that the volatility contains jumps or is even a pure jump process, smoothness of volatility is a fairly common assumption, see Fan and Yao (1998), Kogure (1996), Stanton (1997)). The key tool for the analysis of trajectories of volatility within the framework of functional data analysis (FDA) is functional principal component analysis. Following the Karhunen-Loève representation of the functional volatility process, all functional volatility data can be characterized by their mean function and the eigenfunctions of the autocovariance operator. Hence, each individual trajectory of volatility can be represented by its functional principal component scores. Details of the method are given in the Appendix.

According to Sen (2009), we center the log return process y_t by subtracting the daily mean \bar{y}_t . Alternatively, one could estimate individual drifts by smoothing scatterplots $\{(t_j, y_{t_j}), j = 1, \dots, [1/\Delta]\}$, or kernel smoothers for each day. Denoting the demeaned trajectories obtained from this step by y'_t , we model the intraday variance as follows:

$$Z_{t_j} = \log(\{y'_{t_j}\}^2) - q_0 = V_{t_j} + U_{t_j} \quad (13)$$

where V is the functional volatility process and U_{t_j} has the following properties:

$$\mathbb{E}(U_{t_j}) = 0, \quad \text{Var}(U_{t_j}) = \sigma_U^2, U_{t_i} \perp U_{t_j} \quad \text{for } i \neq j, \quad U \perp V. \quad (14)$$

Note that the constant term $q_0 = 1.27$ guarantees a nondegenerate distribution for U with $\mathbb{E}(U) = 0$. Details on functional data analysis for volatility is given in the appendix.

For each day t , we calculate

$$\Xi_t = \sum_{j=1}^{[1/\Delta]} \left[\exp(Z_{t_j}) - \left(1 + \frac{\sigma_U^2}{2}\right) \exp(V_{t_j}) \right] \quad (15)$$

Conditioning on the V process and the properties of the U process in (14), one can obtain the results for the first two moments of Ξ_t by applying the delta method:

$$\mathbb{E}(\Xi_t) = 0 \quad (16)$$

$$\text{Var}(\Xi_t) = \exp(V_t)^T G_V \exp(V_t) + \frac{\sigma_U^4}{4} \text{Var}(y'_t) \quad (17)$$

Where V_t is estimated by the functional principal components, G_V is the smoothed covariance of V .

Following Barndorff-Nielsen and Shephard (2006), we calculate $\text{Var}(y'_t)$ can be estimated using $\frac{TP_t}{2[1/\Delta]}$.

As Δ goes to zero, under the null hypothesis of no jumps, the asymptotic distribution of the jump test statistics

$$z_{FDA,t} = \frac{\Xi_t}{\sqrt{\exp(V_t)^T G_V \exp(V_t) + \frac{\sigma_U^4 TP_t}{8[1/\Delta]}}} \quad (18)$$

follows a standard Normal distribution.

We detect the days for which this ratio exceeds a preset $1 - \alpha$ quantile of the standard normal distribution to have jumps. Based on the FDA method, we are able to separate the different volatility components that contribute to the realized volatility. Moreover, this method takes into account of the microstructure noise and allows us to test for the jump occurrence.

2.5 Decomposition of Realized Volatility

In many applications, BNS_t contributes to the smooth component of daily realized volatility and the difference $RV_t - BNS_t$ is evidently referred as a consistent estimator for the jump component in the realized variance.

Following a similar logic, using the FDA method we can decompose the RV into three components: smooth volatility, jumps and the variation due to the noise. Note that the first term in the summand in Equation 15 is scaled realized variance. The second term consists of the smooth volatility component $\sum_{j=1}^{[1/\Delta]} [\exp(V_{t_j})]$ scaled with the average level of microstructure noise $(1 + \frac{\sigma_U^2}{2})/\Delta$. For days without jumps, the microstructure noise component is estimated by $\sum_{j=1}^{[1/\Delta]} [\exp(U_{t_j})]$. For days with jump, it is measured by the average level and the jump component is measured by the difference $\sum_{j=1}^{[1/\Delta]} [\exp(U_{t_j})] - \frac{1}{\Delta}(1 + \frac{\sigma_U^2}{2})$.

3 Simulation Study

In this section we carry out a simulation study to evaluate and compare the performance of different jump test statistics. In particular, we test how robust each method would be in response to different model specifications and error distributions.

3.1 One and Two Factor Diffusion Models

As in Huang and Tauchen (2005), we generate *log* prices (p_t) by a one- and two-factor diffusion models.

Single-factor model:

$$dp_t = \mu dt + e^{\beta_0 + \beta_1 v_t} dW_{pt} \quad (19)$$

$$dv_t = \alpha v_t dt + \rho dW_{pt} + \sqrt{1 - \rho^2} dW_t \quad (20)$$

Two-factor model with volatility feedback:

$$dp_t = \mu dt + e^{\beta_0 + \beta_1 v_{1t} + \beta_2 v_{2t}} (\sqrt{1 - \rho_1^2 - \rho_2^2} dW_{pt} + \rho_1 dW_{1t} + \rho_2 dW_{2t}) \quad (21)$$

$$dv_{1t} = \alpha_1 v_{1t} + dW_{1t} \quad (22)$$

$$dv_{2t} = \alpha_2 v_{2t} + (1 + \beta_v v_{2t}) dW_{2t} \quad (23)$$

Specifically, we first generate p_t by the first-order Euler scheme with a time increment of one second per tick. All the other parameter settings are chosen so as to agree with the values presented in Table 1-2 of Huang and Tauchen (2005), i.e. $\mu = 0.03, \alpha = -0.1, \rho = -0.62, \beta_0 = 0, \beta_1 = 0.125$ for the one-factor model (19); $\mu = 0.03, \beta_0 = -1.2, \beta_1 = 0.04, \beta_2 = 1.5, \alpha_1 = -0.0014, \alpha_2 = -1.386, \beta_v = 0.25, \rho_1 = \rho_2 = -0.3$ for the two-factor model (21). Second, we perturb each p_t by a noise term u_t to create the 'observed' price level p_t^o :

$$p_t^o(t_j) = p_t(t_j) + u_t(t_j) \quad (24)$$

We assume that u_t is an identically independent process generated from either a Normal distribution $u_t(t_j) \sim N(0, \sigma_{mn}^2)$ or an Extreme Value distribution $u_t(t_j) \sim EVT(0, \sigma_{mn}^2)$.

For each method, namely, bipower variation (z_{BNS}), bipower variation with staggered returns (z_{HT}), scale variation (z_{AS-J}) and functional data analysis (z_{FDA}), we conduct a right-tailed test at nominal level $\alpha = 1\%$. Following Aït-Sahalia and Jacod (2009), we choose $\gamma = 4$ and $k = 2, 3, 4$ in equation (12) to allow more emphasis on large jumps in price process and compare the behaviors of the fourth-power variations as k increases. We use the upper 99% critical value of the standard Gaussian distribution as cut-off values. From the simulations, we check the percentage of samples that have test statistics higher than the critical value. We call this the empirical rejection rate (ERR) of the test:

$$ERR = \frac{\sum_{i=1}^n \mathbf{1}_{z \geq z_\alpha}}{n} \quad (25)$$

If the ERR of a test is larger than its nominal level, then it is making too many type I errors. That means, such a test is falsely detecting too many days as having jumps. Table 1-2 present the ERR of tests based on the different methods.

First, for all data generating processes and microstructure noise distributions we consider, we find that the size of noise has a significant impact on the ERR of the z_{BNS} . As σ_{mn} increases, the ERR of z_{BNS} decreases under both noise structures.

However, this pattern does not hold for z_{HT} . Second, as z_{HT} is mainly derived to help restore the ERR of z_{BNS} , it tends to be oversized, which might lead to detect spurious jumps when the underlying process contains no jump. Note that this is more pronounced when the noise distribution is EVT. Third, in the two-factor model, both z_{BNS} and z_{HT} have very high ERR without any microstructure noise. This is not surprising since, according to Chernov et. al. (2003) and Huang and Tauchen (2005), the two-factor stochastic volatility model with volatility feedback could generate sudden and large price movements. Both z_{BNS} and z_{HT} would falsely detect these as jumps. For both data generating processes, the ERR's of z_{AS-J} at various levels of k are all much above 1% level, which would overreject the null hypothesis of no jumps in the underlying process. Finally, we find that the ERR of the z_{FDA} is very robust to different size and distribution of the noise. Moreover, it has a better ERR for a two-factor model when the observed prices are equal to the true prices. In summary, the ERR of z_{FDA} is very close to the nominal level of the test for all data generating processes and microstructure noise distributions.

3.2 Autocorrelated Returns

Since nonsynchronous trading may induce serial correlation in the sequence of observed price changes, we study the power of each jump detection method (z -statistics, namely z_{BNS} , z_{HT} and z_{FDA}) using simulated data on $lag = 1$ autocorrelated returns.

Consider the simple model in Roll (1984), the observed price and efficient price levels are differentiated by the bid-ask spread:

$$p_t^o(t_j) = p_t(t_j) + I_t(t_j) \frac{S}{2} \quad (26)$$

where $S = p_a - p_b$ is the bid-ask spread, $I_t(t_j)$ is an order-type indicator, which takes a value of 1 with probability 0.5 signifying buyer-initiated transaction or -1 with probability 0.5 as a seller-initiated transaction:

The efficient price p_t levels are simulated based on (19) and (21). According to Bandi and Russell (2008), we set $S = 0.018$ in this simulation such that the $lag = 1$ autocorrelation of the 1-minute return is -0.12 .

Table 1-2 present the ERR based on the bipower variation, scale variation and FDA jump detection methods when the simulated returns are autocorrelated. In one-factor SV model, the ERR of both HT and BNS methods is higher than the nominal level at 1%. Whereas, the ERR based on the FDA method matches the nominal level at 1%. The ERR based on AS-J method is much higher than the nominal level at all parameter settings. This suggests that the bipower variation methods tend to detect spurious jumps when there is no jump in the underlying process. For the two-factor SV model, the ERR levels based on both z_{HT} and z_{BNS} tend to be more oversized compared at 1% significance level. This is consistent with our previous finding when the noise is assumed to be independent. The ERR based

on AS-J method is pretty close to the nominal level at some parameter settings. This is the only scenario where the AS-J performs well.

4 Empirical Applications

In the rest of the paper, we evaluate the ability of the competing volatility separation methods to predict future volatility dynamics. In particular, we make prediction and forecast of the Value at Risk (VaR) and Expected Shortfall (ES) of the exchange rate return distribution. The VaR and ES are often used to measure extreme market risks, hence they are closely related to the jumps. Our second application is to revisit the issue of unbiasedness between the implied volatility and future integrated volatility and examine how each realized variation measure can play a role to explain this issue.

4.1 Data

Our empirical applications are conducted using the 5-minute high-frequency data on Japanese Yen to Euro (JPY/EUR) and US to Euro Dollar (USD/Euro) from March 1, 1990 to July 31, 2006. The intraday price quotes span the time interval from 00:00 through 23:55 (GMT), which yields 288 observations per day. We discard days with less than 240 data entries and fill in the missing values using linear interpolation method. Our options data consists of the at-the-money (ATM) 1-month implied volatilities of JPY/EUR and USD/EUR from December 6, 1992 to July 31, 2006. Table 3 summarizes the sample statistics of our data.

4.2 Bias in Test Statistics Distribution

Our main idea is to assess validity of the proposed FDA method to separate the realized variance of exchange rates into a smooth volatility, jump and microstructure noise components. Figure 1 presents the kernel densities of the JPY/EUR and USD/EUR test statistics calculated by, respectively, the non-parametric FDA, the bipower variation with staggered returns, and the standard bipower variation methods. We show that these empirical distributions have positive bias relative to the standard normal. It is expected that this pattern would become even more pronounced when the sampling frequency is higher because the bias is mainly due to the variation of microstructure noise. For the FDA method, the sampling frequency should not affect the distribution too much. To summarize, it is clear that the non-parametric FDA method provides a more consistent result with the asymptotic conclusion in section 2 that z_{FDA} follows the standard normal distribution.

5 VaR Application

For the returns on a given investment portfolio over a certain holding period, a risk manager who wants to assess a market risk of a given portfolio is mainly concerned with a potential loss, which is caused by extreme market movements. VaR is a value that is commonly used to measure the probability of such portfolio losses at a certain confidence level. In mathematics, VaR is referred as a quantile in the return distribution.

Among the existing literature for quantile forecasts using high-frequency returns, a general approach to forecast VaR is taken in two steps. The first task is to identify and estimate a time series model for the volatility forecasts. The second step is to evaluate the empirical return distribution and obtain VaR forecasts from the volatility forecasts. As shown in Andersen, Bollerslev and Diebold (2007), most of the predictable variation in daily realized volatility comes from its strongly persistent smooth component, while the predictability of the jumps becomes rather minor. In this section, our main focus for the first step is to model each realized variation measure based on different separation method mentioned before for the volatility forecasts. We want to analyze how these variation measures contribute to the VaR forecasts. Our second task is a straightforward application of the empirical finding in Andersen et. al. (2000) that the empirical distribution of the standardized exchange rate returns can be closely approximated by a standard normal.

5.1 VaR in-sample prediction

Denote FDV_t to be a smooth variance component estimated by the FDA method

$$FDV_t = \exp(q_0) \left(1 + \frac{\sigma_W^2}{2} \right) \sum_{j=1}^{[1/\Delta]} \exp(V_{tj}) + [1/\Delta] \bar{y}_t^2 \quad (27)$$

Note that the FDA method is implemented with the centered returns, therefore, the second term in equation (27) is to adjust FDV_t so that it can be evaluated with the other realized variation measures in the same scale. It is expected that FDV_t is mostly higher than BNS_t and HT_t , because by its construction, FDV_t is scaled by multiplying the smooth variation of intraday returns with the average level of microstructure noise; whereas BNS_t and HT_t are used to measure only the smooth intraday return variation.

Figure 2 and 3 present the QQ plots of the standardized daily JPY/EUR and USD/EUR returns using RV_t , FDV_t , BNS_t and HT_t . Each plot focuses on the left tail of the sample distribution, indicating that the FDV -adjusted returns can be closely distributed as a standard normal. Moreover, Giot and Laurent (2004) shows how to achieve better VaR forecasts based on skewed student distribution. Following Giot and Laurent (2004), we estimate the parameter of skewness (ξ) and parameter of

kurtosis (ν) in the skewed student t distribution based on the standardized returns by realized variance measures. We find that the MLE estimates of ξ on both JPY/EUR and USE/EUR are very close to 1 (For example, $\xi = 1.0085$ for JPY/EUR and $\xi = 1.0095$ for USD/EUR), indicating that the distribution of standardized returns are very symmetric.

Let $x_{t,\alpha}$ be the α -quantile of the return distribution for day t :

$$x_{t,\alpha} = \inf\{x \in \mathbf{R} : F_t(x) \geq \alpha\} \quad (28)$$

According to Andersen et. al. (2000) and Giot and Laurent (2004), we assume that the exchange rate return quantile $x_{t,\alpha}$ follows:

$$x_{t,\alpha}^v = \mu + \sqrt{v_t} z_\alpha \quad (29)$$

where $v_t = \{RV_t, FDV_t, HT_t, BNS_t\}$ are the variation processes of the returns and z_α is the α -quantile in a standard normal distribution or a standard student distribution.

Now we define the level of ERR:

$$ERR(x_{v,\alpha}) = \frac{\sum_{t=1}^T \mathbf{1}_{y_t \leq x_{t,\alpha}^v}}{T} \quad (30)$$

The upper panels in Table 4 and 5 present the difference in percentage between the ERR calculated in equation (30) and the predetermined significance levels (1% and 99%). We find that estimating VaR quantiles based on the FDA method provides the closest match to the nominal level of 1%. The estimated VaR based on both BNS and HT methods seem biased upward at the lower 1% level and biased downward at upper 99% quantiles of a standard normal distribution. However, we show that these biases can be corrected when the quantiles are determined based on a standard student t distribution in equation (28).

5.2 One-day ahead forecast of VaR

In this section, we discuss the ERR of the one-day ahead VaR forecast

$$x_{t|t-1,\alpha}^v = E(x_{t,\alpha}|v_{t-1}), \quad v_{t-1} = \{RV_{t-1}, FDV_{t-1}, HT_{t-1}, BNS_{t-1}\} \quad (31)$$

We use the first half of our sample (T') to estimate the time series model for each v process. With the second half sample, we evaluate the ERR of the VaR forecast based on the forecast of each v . We consider the following ARFIMA(p, d, q) model to fit the process of $v_t, t = 1, \dots, T'$:

$$(1 - L)^d v_t = \phi_0 + \sum_{j=1}^p \phi_j v_{t-j} + u_t \quad (32)$$

Where u_t is assumed to be iid normally distributed. Note the value of p is determined by the partial autocorrelations of each v series; the value of d is estimated by the standard Geweke and Porter-Hudak (1983) method.

For each $t \in [T' + 1, T]$, $v_{t|t-1}$ can be readily computed based on the parameter estimates in equation (32). Hence, a VaR forecast conditioning on $v_{t|t-1}$ can be estimated as follows:

$$x_{t|t-1,\alpha}^v = \mu + \sqrt{v_{t|t-1}}z_\alpha, \quad t \in \{T' + 1, \dots, T\} \quad (33)$$

Finally, we move the estimation window one day forward and repeat the above procedure.

We calculate the ERR level as:

$$ERR(x_{v,\alpha}) = \frac{\sum_{t=T'+1}^T \mathbf{1}_{y_t \leq x_{t|t-1,\alpha}^v}}{T - T'} \quad (34)$$

The second panels in Table 4 and 5 report that the *FDV*-based VaR forecast outperforms those with other variation measures according to the standard normal distribution in equation (33). Also, we find that the biases in the VaR forecasts can be corrected by using the standard student t distribution in equation (33). In a long-memory model framework, we show that the *FDV* measure provides the most accurate VaR forecasts according to the standard normal distribution. We also note that the autoregressive order of p is substantially reduced for each realized variation process in a long-memory model with the estimated degree of integration d ranged between $0.3 < d < 0.4$.

6 Expected shortfall application

Although VaR is often used as a standard tool for evaluating financial market risk, it disregards the potential overall losses beyond the VaR quantile. To overcome this drawback of VaR, an alternative risk measure, termed Expected shortfall (ES), has become gradually recognized in both academia and practice. In general, ES is defined as the conditional expectation of the returns that exceed the VaR.

Following the procedure of modeling each v process in the previous section, we continue to look at the unconditional distributions of the exchange rate returns standardized by v . In particular, our concern is to learn how well the (left) tail behavior of these empirical distributions be approximated by a standard normal.

According to each estimates of $v_{t|t-1}$ from the previous section, we first adjust the raw returns as follows:

$$\hat{z}_t^v = \frac{y_t}{\sqrt{v_{t|t-1}}}, \quad v = \{RV, FDV, BNS, HT\} \quad (35)$$

then compute ES_α :

$$ES_\alpha = \frac{\sum \hat{z}_t^v \mathbf{1}_{\hat{z}_t^v \leq \hat{z}_\alpha^v}}{\sum \mathbf{1}_{\hat{z}_t^v \leq \hat{z}_\alpha^v}}, \quad t = T' + 1, \dots, T. \quad (36)$$

where $\{\hat{z}_t^v\}$ is the v -standardized returns and \hat{z}_α^v is the α -th order statistic of $\{\hat{z}_t^v\}$.

Using the ES value of -2.6426 as our benchmark, as it corresponds to the ES at 1% percentile of a standard normal distribution, Table 6 shows that the expected total losses (gains) that correspond to the 1% empirical percentile of the standardized returns based on the FDA method provide the closest match with the benchmark. This suggests that the unconditional distribution of the *FDV*-adjusted exchange rate returns can be better approximated by a normal distribution.

7 Forecasting Realized Variance by Decomposition

Andersen, Bollerslev and Diebold (2007) shows that decomposing total return variability into continuous and jump components improves volatility forecasts. Lanne (2007) argues that the potential gain in forecast accuracy is due to the fact that it is easier to capture the continuous volatility process without jumps. In this section, we study whether different methods of decomposition affect the realized volatility forecasting.

Define continuous (C) and jump (J) sample path volatility component as:

$$C_{t,\alpha,v} = I[z_{t,v} \leq z_\alpha]RV_t + I[z_{t,v} > z_\alpha]v_t \quad (37)$$

$$J_{t,\alpha,v} = I[z_{t,v} > z_\alpha], \quad v = \{FDV, HT, BNS\} \quad (38)$$

where $I(\cdot)$ denotes the indicator function and $z_{t,v}$ is the empirical z statistics based on different realized variance measure v .

Following Andersen, Bollerslev and Diebold (2007) we use a simple-to-estimate ARMA model for one-day ahead volatility forecasts. According to Tsay and Tiao (1984), we select an ARMA($p = (1, 5), q = (1, 2, 6)$) that can best describe the *log* realized variances of both JPY/EUR and USD/EUR series.

$$\log(RV_{t+1}) = \phi_0 + \phi_1 \log(RV_t) + \phi_2 \log(RV_{t-4}) + \epsilon_{t+1} + \theta_1 \epsilon_t + \theta_2 \epsilon_{t-1} + \theta_3 \epsilon_{t-5} \quad (39)$$

Figure 4 displays the ACF plots based on the residuals. The p -values of the Ljung-Box statistic are 0.0756 for JPY/EUR and 0.7908 for USD/EUR.

Given the separated smooth volatility and jump components² of the realized variance, we modify equation (39) to forecast RV with the two components:

$$\begin{aligned} \log(RV_{t+1}) &= \phi_0 + \phi_1 \log(C_{t,v}) + \phi_2 \log(C_{t-4,v}) + \phi_3 \log(1 + J_{t,v}) \\ &+ \epsilon_{t+1} + \theta_1 \epsilon_t + \theta_2 \epsilon_{t-1} + \theta_3 \epsilon_{t-5}, \quad v = \{FDV, HT, BNS\} \end{aligned} \quad (40)$$

We take the first half ($t = 1, \dots, T'$) of JPY/EUR and USD/EUR for the ML estimation and generate one-day-ahead forecasts to compare with the second half of the RV observations on both series. To improve our forecast accuracy, we also adopt the rolling sample method as suggested in Andreou and Ghysels (2001). Specifically, we evaluate each daily RV forecast by discarding the first observation and including the most recent observation in each estimation sample in equation (41) and (42) at each $\tau = T', \dots, T - 1$.

$$\begin{aligned} \log(RV_{t+1}) &= \phi_{0,\tau} + \phi_{1,\tau} \log(RV_t) + \phi_{2,\tau} \log(RV_{t-4}) \\ &+ \epsilon_{t+1} + \theta_{1,\tau} \epsilon_t + \theta_{2,\tau} \epsilon_{t-1} + \theta_{3,\tau} \epsilon_{t-5} \end{aligned} \quad (41)$$

$$\begin{aligned} \log(RV_{t+1}) &= \phi_{0,\tau} + \phi_{1,\tau} \log(C_{t,v}) + \phi_{2,\tau} \log(C_{t-4,v}) + \phi_{3,\tau} \log(1 + J_{t,v}) \\ &+ \epsilon_{t+1} + \theta_{1,\tau} \epsilon_t + \theta_{2,\tau} \epsilon_{t-1} + \theta_{3,\tau} \epsilon_{t-5}, \quad v = \{FDV, HT, BNS\} \end{aligned} \quad (42)$$

To obtain statistical significance on forecast accuracy, we use the forecast errors by equation (39) and (41) as the benchmark and report the results of pairwise test statistic according to Diebold and Mariano (1995). Diebold and Mariano (DM) test is proposed to compare forecasting performances based on two models. Let d be the difference of the squared forecast errors based on the two models:

$$d_v = e_v^2 - e_{RV}^2, \quad v = \{BNS, FDV, HT\} \quad (43)$$

$$\begin{aligned} \frac{\bar{d}_v}{\sqrt{\frac{\hat{V}(\bar{d}_v)}{T}}} &\sim \mathbf{N}(0, 1), \\ \hat{V}(\bar{d}_v) &= \hat{V}_0 + \sum_{j=1}^J \omega(j) \left[\hat{V}_j + \hat{V}'_j \right], \\ \hat{V}_j &= \frac{1}{T} \sum_{t=j+1}^T (d_{v,t} - \bar{d}_v)(d_{v,t-j} - \bar{d}_v)' \end{aligned}$$

²Note that the jump size is omitted in the model since we find that including the jump occurrence alone and the continuous component provide better forecasts for the realized variance.

where $\omega(\cdot)$ is a decaying function in j with J set as a truncation parameter³.

Note that a significantly negative test statistics indicates that forecasting RV based on the continuous volatility and jump components outperforms using lags of RV alone.

For the series of USD/EUR, the test statistics in Table 7 indicate that at 1% significance level, out-of-sample forecasts based on the separated continuous volatility and jump components are considerably more accurate than modeling realized variance based on its own path. This finding is in line with Andersen, Bollerslev and Diebold (2007) and Lanne (2007).

Table 8 shows in-sample estimation results for equation (40) based on different decomposition methods. It is important to note that the coefficient estimates of the jump component are significantly positive based on both FDA and HT methods. This means that the impact of their lagged continuous component is considerably enlarged by the jump component. For JPY/EUR, one would expect an averaged $0.9155 + 0.0638/5 = 0.9283$ by FDA method or $0.8488 + 0.1149/5 = 0.8718$ by HT method units of increase on the next day's $\log RV$ forecast given a unit increase in the corresponding \log continuous component on days with no jumps. But for days with jumps, the $\log RV$ forecasts are predicted to increase by $0.6033 * \log(2) = 0.4181$ by FDA method and $0.416 * \log(2) = 0.2883$ by HT method. For USD/EUR, the results are very similar showing that the impact of lagged continuous RV component on the next day's $\log RV$ forecast is significantly increased by the jumps detected using FDA or HT method.

8 The Relation Between Implied Volatility and Realized Volatility

Implied volatility ($IV_{t,t+\tau}$) is known as a time- t volatility measure inverted from an option price through Black-Scholes formula, where τ is the time-to-maturity of the contract. Moreover, option price is often directly quoted by IV , for example, in the over-the-counter (OTC) markets.

The VaR application discussed in previous section is heavily hinging upon the jump component. However, IV is often viewed as a perfect predictor for the future integrated volatility. Hence, IV should be crucially related to the smooth (continuous) part of the daily volatility. A number of studies have been dedicated to empirically test for the information content of IV and its forecasting power for future volatility in the forecasting regression framework:

$$INTV_{t,t+\tau} = \alpha + \beta IV_{t,\tau} + \epsilon_t \quad (44)$$

³We set $J = 0$ in this paper.

where $INTV_{t,t+\tau}$ is the annualized τ -day moving average of the integrated realized volatility:

$$INTV_{t,t+\tau} = \sqrt{\frac{252}{\tau} \sum_{j=0}^{\tau} v_{t+j}} \quad (45)$$

In the absence of volatility risk premium, Hull and White (1987) indicates that IV is expected to be an unbiased forecast of future integrated volatility, *i.e.*

$$IV_{t,\tau} \approx E_t^Q (INTV_{t,t+\tau}) \quad (46)$$

We compare the forward-looking performance of IV for the integrated volatility based on $v = \{RV, FDV, BNS, HT\}$. We adopt the GMM estimation method to conduct a Likelihood Ratio (LR) test on a joint restrictions of $\alpha = 0, \beta = 1$ in (44). We preselect just-identified moment conditions and use Newey-West kernel (1987) in order to obtain more robust standard errors to the serial correlations in the sample moment conditions ⁴.

$$E [(INTV_{t,t+\tau} - \alpha - \beta_{IV} IV_{t,\tau}) \times Z_t] = 0 \quad (47)$$

Where the instrumental variables $Z_t = [1, IV_{t,\tau}]$.

Table 9 presents our forecasting regression results. For both JPY/EUR and USD/EUR exchange rate series, IV provides the best power in predicting the integration of future FDV measure. We find that the restrictions of $\alpha = 0, \beta = 1$ are rejected through all v . Moreover, we find that the estimates of β are greater than 1 with JPY/EUR while they are smaller than 1 with USD/EUR series.

9 Conclusions

In the presence of microstructure noise, we examine jump test statistics for detecting days on which a price process displays jumps using high-frequency data. In particular, we compare the Empirical Rejection Rate (ERR) of different proposed test statistics in the applications of VaR, Expected shortfall, forecasting realized variance, and implied volatility. The test statistics considered are based on power variation, scale variation and principal component analysis of the functional data. The last non-parametric procedure provides a tool for separating different components that contribute to the total daily realized volatility. The results demonstrate that the volatility measure based on the functional data estimation method provides better predictive ERR for the VaR return quantiles as well as the ES. Also, FDA method is shown to outperform bipower variation methods in the application of VaR

⁴The test statistics is implemented by the difference in the restricted and unrestricted objective functions multiplied by the sample size, note that the restricted model is estimated using the same weighting matrix as the unrestricted model.

forecast. In modeling for realized volatility forecasts, our estimation results coincide with Andersen, Bollerslev and Diebold (2007) and Lanne (2007) that it is important to explicitly allow for continuous volatility and jump components in RV forecasting model. Moreover, we find that different separation methods offer varying levels of forecast accuracy. In our last application, we find that at-the-money implied volatility is able to better fit the future smoothed volatility estimated by the FDA method. In summary, the FDA method outperforms bipower variation based method in all three practical applications.

Appendix: Details of Principal Components Analysis of Functional Data for Volatility Trajectories

Consider the general class of models for asset prices driven by the stochastic differential equation

$$d\log P(t, \omega) = \tilde{\mu}(t, \omega) dt + \tilde{\sigma}(t, \omega) dW(t, \omega), \quad t \geq 0. \quad (48)$$

Here $\tilde{\mu}(t, \omega)$, $\tilde{\sigma}(t, \omega)$ are not necessarily stationary stochastic processes, and W is a Wiener process. One does not actually observe continuous data and it is therefore necessary to consider discretized versions, defining scaled log-returns and associated diffusion terms

$$\begin{aligned} Y_{\Delta} &= \frac{1}{\sqrt{\Delta}} \log \left(\frac{P(t + \Delta)}{P(t)} \right), \\ W_{\Delta} &= \frac{1}{\sqrt{\Delta}} (W(t + \Delta) - W(t)). \end{aligned}$$

For small Δ one arrives at the approximate model

$$Y_{\Delta}(t) \approx \tilde{\sigma}(t) W_{\Delta}. \quad (49)$$

This implies

$$\log Y_{\Delta}^2 = \log \tilde{\sigma}(t)^2 + \log(W_{\Delta})^2 \quad (50)$$

which is same as equation (13) with $E\log(W_{\Delta})^2 = q_0 = 1.27$

Trades are assumed to be recorded on a dense discrete time grid $t_j = j\Delta$, $j = 1, 2, \dots, [T/\Delta]$. The empirical observations $Y_{ij\Delta}$ are the transaction recordings contaminated by independent non-negative errors $e_{ij} > 0$. Specifically,

$$\tilde{Y}_{ij\Delta} = \frac{1}{\sqrt{\Delta}} \log \left(\frac{P_i(t_j + \Delta)}{P_i(t_j)} \right) e_{ij}, \quad i = 1, \dots, n, \quad j = 1, \dots, [T/\Delta]. \quad (51)$$

Our target for inference is the smooth process V defined by

$$V(t) = \log(\{\tilde{\sigma}(t)\}^2). \quad (52)$$

We refer to V as *functional volatility process*.

We represent the smooth functional V in terms of its decomposition into functional principal components, a common approach in FDA. For a domain \mathcal{T} , setting

$$G_V(s, t) = \text{cov}(V(s), V(t)), \quad E(V(t)) = \mu_V(t), \quad s, t \in \mathcal{T}, \quad (53)$$

the functional principal components are the eigenfunctions of the auto-covariance operator $G_V : L^2 \mapsto \mathbb{R}$, a linear operator on the space L^2 of functions V , that is given by

$$\mathbf{G}_V(g)(s) = \int_{\mathcal{T}} G_V(s, t)g(t) dt. \quad (54)$$

We denote the orthonormal eigenfunctions by ϕ_k , with associated eigenvalues λ_k for $k = 1, 2, \dots$, such that $\lambda_1 \geq \lambda_2 \geq \dots$ and $\sum_k \lambda_k < \infty$. The Karhunen-Loève theorem (see Rice and Silverman (1991)) provides a representation of individual random trajectories of the functional V , given by

$$V(t) = \mu_V(t) + \sum_{k=1}^{\infty} \xi_k \phi_k(t), \quad t \in \mathcal{T} \quad (55)$$

where the ξ_k are uncorrelated random variables that satisfy

$$\xi_k = \int (V(t) - \mu_V(t))\phi_k(t) dt, \quad E\xi_k = 0, \quad \text{var}(\xi_k) = \lambda_k. \quad (56)$$

Under the data generating mechanism in (51), one has

$$E(Y_{\Delta}(t)) = \mu_V(t), \quad \text{cov}(Y_{\Delta}(s), Y_{\Delta}(t)) = O(\sqrt{\Delta}) + G_V(s, t) \quad \text{for } |t - s| \geq \Delta. \quad (57)$$

This implies that the smooth mean function μ_V and the smooth covariance surface G_V can be consistently estimated from available data, by pooling the sample of n trajectories and smoothing the resulting scatterplot. The exception for targeting points on G_V with $|t - s| < \Delta$ in (57), that is necessitated by the dependence of the increments of W for overlapping intervals $[t, t + \Delta] \cap [s, s + \Delta] \neq \emptyset$, does not pose a problem, since it follows from $\Delta \rightarrow 0$ and the smoothness of the surface G_V that the areas of $G_V(s, t)$, for which $|t - s| < \Delta$, can still be consistently estimated. Well-known procedures exist to infer eigenfunctions and eigenvalues (Rice and Silverman (1991); Müller et al. (2007)). At the core of the estimation procedure is the principal analysis of random trajectories (PART), applied to the data, which is an algorithm to obtain mean and eigenfunctions, as well as FPC scores, from densely sampled functional data, as described in Müller et al. (2007). The smoothing steps in this algorithm are implemented with weighted local linear smoothing (Fan and Gijbels, 1996), which works well in practice; alternative smoothing methods can also be used.

Processes V are then approximated by substituting estimates and using a judiciously chosen finite number K of terms in the sum for representation (55). This choice can be made using one-curve-leave-out cross-validation (Rice and Silverman (1991)), pseudo-AIC criteria (Yao et al. (2005)) or a scree plot, a tool from multivariate analysis, where one uses estimated eigenvalues to obtain a prespecified fraction of variance explained as a function of K or looks for a change-point.

References

- Aït-Sahalia, Y., P.A. Mykland and L. Zhang (2005) 'How Often to Sample a Continuous-Time Process in the Presence of Market Microstructure Noise', *Review of Financial Studies*, 18, 351-416.
- Aït-Sahalia, Y. and J. Jacod (2009) 'Testing for Jumps in a Discretely Observed Process', *Annals of Statistics*, 37, 184-222.
- Andersen, T. G. and T. Bollerslev(1998), 'Answering the Skeptics: Yes, Standard Volatility Models Do Provide Accurate Forecasts', *International Economic Review*, 39, 885-905.
- Andersen, T. G., T. Bollerslev, F. X. Diebold and P. Labys (2000), 'Exchange Rate Returns Standardized by Realized Volatility are (Nearly) Gaussian', *Multinational Finance Journal*, 4, 159-179.
- Andersen, T. G., T. Bollerslev, F. X. Diebold and P. Labys (2003), 'Modelling and Forecasting Realized Volatility', *Econometrica*, 71, 579-625.
- Andersen, T. G., T. Bollerslev and N. Meddahi (2004), 'Analytical Evaluation of Volatility Forecasts', *International Economic Review*, 45, 1079-1110.
- Andersen, T. G., T. Bollerslev and F. X. Diebold (2007), 'Roughing It Up: Including Jump Components in the Measurement, Modeling and Forecasting of Return Volatility', *Review of Economics and Statistics*, 89(4), 701-720.
- Andreou E. and E. Ghysels (2001), 'Rolling-Sample Volatility Estimators: Some New Theoretical, Simulation and Empirical Results', *Journal of Business and Economic Statistics*, 20, 363-376.
- Bandi, F.M. and J.R. Russell (2006), 'Separating Microstructure Noise from Volatility', *Journal of Financial Economics*, 79(3), 655-692.
- Bandi, F.M. and J.R. Russell (2008), 'Microstructure Noise, Realized Variance, and Optimal Sampling', *Review of Economic Studies*, 75, 339-369.
- Barndorff-Nielsen, O. E. and N. Shephard (2002), 'Econometric Analysis of Realized volatility and its Use in Estimating Stochastic Volatility Models', *Journal of Royal Statistical Society(B)*, 64, 253-280.
- Barndorff-Nielsen, O. E. and N. Shephard (2003), 'Realized Power Variation and Stochastic Volatility', *Bernoulli*, 9, 243-265.

- Barndorff-Nielsen, O. E. and N. Shephard (2004), 'Power and Bipower Variation with Stochastic Volatility and Jumps (with discussion)', *Journal of Financial Econometrics*, 2, 1-48.
- Barndorff-Nielsen, O. E. and N. Shephard (2006), 'Econometrics of Testing for Jumps in Financial Economics using Bipower Variation', *Journal of Financial Econometrics*, 4(1), 1-30.
- Barndorff-Nielsen, O. E., P. R. Hansen, A. Lunde and N. Shephard (unpublished manuscript) 'Designing realised kernels to measure the ex-post variation of equity prices in the presence of noise'.
- Bollerslev, T. (1986), 'Generalized Autoregressive Conditional Heteroskedasticity', *Journal of Econometrics*, 31, 307-327.
- Chernov, M., A. R. Gallant, E. Ghysels and G. Tauchen (2003), 'Alternative Models of Stock Price Dynamics', *Journal of Econometrics*, 116, 225-257.
- Clark, P. K. (1973), 'A Subordinated Stochastic Process Model with Finite Variance for Speculative Prices', *Econometrica*, 41, 135-155.
- Diebold, F.X. and R.S. Mariano (1995) 'Comparing Predictive Accuracy', *Journal of Business and Economic Statistics*, 13, 253-263.
- Engle, R. (1982), 'Autoregressive Conditional Heteroskedasticity with Estimates of the Variance of United Kingdom Inflation', *Econometrica*, 50, 987-1007.
- Fan, J. and Q.W. Yao (1998) 'Efficient estimation of conditional variance functions in stochastic regression' *Biometrika*, 85, 645-660.
- Fan, J. and Y. Wang (2007) 'Multi-Scale Jump and Volatility Analysis for High-Frequency Financial Data', *Journal of American Statistical Association*, 102(December): 1349-1362.
- Gallo, G. M. and M. Velucchi (2007) 'On the Interaction between Ultra-High Frequency Measures of Volatility' *Universita' di Firenze, Dipartimento di Statistica Econometrics Working Paper No. 2007-01*.
- Geweke, J. and S. Porter-Hudak (1983) 'The Estimation and Application of Long Memory Time Series Econometrics' *Journal of Time Series Analysis*, 4, 221-238.
- Giot, P. and S. Laurent (2004) 'Modelling Daily Value-at-Risk using Realized Volatility and ARCH type models' *Journal of Empirical Finance*, 11-3, 379-398.
- Hansen, P.R. and A. Lunde (2006) 'Realized Variance and Market Microstructure Noise' *Journal of Business and Economic Statistics*, 24(2), 127-161.

- Huang, X. and G. Tauchen (2005) 'The Relative Contribution of Jumps to Total Price Variation' *Journal of Financial Econometrics* 3(4). 456-499.
- Hull, J. and A. White (1987) 'The Pricing of Options on Assets with Stochastic Volatility', *Journal of Finance*, 42. 281-300.
- Jacod, J., Y. Li, P. Mykland, M. Podolskij and M. Vetter (forthcoming) 'Microstructure Noise in the Continuous Case: The Pre-Averaging Approach' *Stochastic Processes and their Applications*
- Jiang, G.J. and R.C.A. Oomen (2008) 'Testing for Jumps When Asset Prices are Observed with Noise - a "Swap Variance" Approach', *Journal of Econometrics*, 144, 352-370.
- Kogure, A. (1996) 'Nonparametric prediction for the time-dependent volatility of the security price', *Financial Engineering Jap. Market* 3, 1-22.
- Lanne, M. (2007) 'Forecasting Realized Exchange Rate Volatility by Decomposition' *International journal of forecasting*, 23(2). 307-320.
- Lee, S., and Mykland, P.A. (2008) 'Jumps in Financial Markets: A New Nonparametric Test and Jump Dynamics', *Review of Financial Studies*, 21, 2535-2563.
- Müller, H.G., R. Sen and U. Stadtmüller (2007) 'Functional data Analysis for Volatility Process' Preprint.
- Oomen, R.C.A. (2005) 'Properties of Bias-Corrected Realized Variance under Alternative Sampling Schemes', *Journal of Financial Econometrics*, 3(4), 555-577.
- Pan, J. (2002) 'The Jump-risk Premia Implicit in Options: Evidence from an Integrated Time-series Study', *Journal of Financial Economics*, 63, 3-50.
- Roll, Richard (1984) 'A Simple Implicit Measure of the Effective Bid-Ask Spread in an Efficient Market', *Journal of Finance*, 39, 1127-1139.
- Sen, R. (2009) 'Jumps and Microstructure noise in Stock Price Volatility.' in *Stock Market Volatility* ed. Greg N. Gregoriou Chapman Hall/Taylor And Francis, 163-180.
- Stanton, R. (1997) 'A nonparametric model of term structure dynamics and the market price of interest rate risk', *J. Finance* 52, 1973-2002.
- Tauchen, G. (2006). 'Realized Jumps on Financial Markets and Predicting Credit Spreads.' *Journal of econometrics*
- Todorov V. and G. Tauchen (Forthcoming) 'Volatility Jumps', *Journal of Business and Economic Statistics*.

Tsay, R. S. and G. C. Tiao (1984) 'Consistent Estimates of Autoregressive Parameters and Extended Sample Autocorrelation Function for Stationary and Non-stationary ARMA models', *Journal of the American Statistical Association*, 79, 84-96.

Zhang, L., P.R. Mykland and Y. Aït-Sahalia (2005) 'A tale of Two Time Scales: Determining Integrated Volatility with Noisy High-Frequency Data', *Journal of the American Statistical Association*, 100, 1394-1411.

Zhou, B. (1996) 'High-Frequency Data and Volatility in Foreign Exchange Rate', *Journal of Business and Economic Statistics*, 14, 45-52.

Table 1: We present the difference (in percentage) between ERR and 1% significance level of the jump statistics under microstructure noise at 5-minute sampling interval. This simulation is based on a single-factor stochastic volatility model. We follow the parameter settings in Huang and Tauchen (2005). The upper panel is for the tests based on bipower variation (BNS), the staggered bipower variation (HT), scale variation (AS-J) and the FDA method with the noise drawn from a Normal distribution $\mathbf{N}(0, \sigma_{mn}^2)$ and the lower panel is for the tests with noise drawn from an extreme value distribution $\mathbf{EVT}(0, \sigma_{mn}^2)$. The values reported are the difference from the nominal level, expressed in percentage.

σ_{mn}	BNS	HT	AS - J ($\gamma = 4$)			FDA
			$k = 2$	$k = 3$	$k = 4$	
0	0.45	0.20	5.15	6.35	6.40	-0.05
	<u>Normal</u>					
0.027	0.20	0.50	7.10	15.20	16.35	-0.05
0.08	-0.65	0.50	11.75	18.95	18.45	-0.05
	<u>EVT</u>					
0.027	0.35	0.15	6.85	14.90	16.50	-0.05
0.08	-0.55	3.35	10.60	17.90	17.60	-0.10
	<u>Autocorrelated Noise</u>					
	0.10	0.15	5.75	13.60	14.80	0.00

Table 2: We present the difference (in percentage) between the ERR and 1% nominal level of the jump statistics under microstructure noise at 5-minute sampling interval. This simulation is based on a two-factor stochastic volatility model with the same parameter settings in Table 2 of Huang and Tauchen (2005). The upper panel is for the tests based on bipower variation (BNS), the staggered bipower variation (HT), scale variation(AS-J) and the FDA method with the noise drawn from a Normal distribution $\mathbf{N}(0, \sigma_{mn}^2)$ and the lower panel is for the tests with noise drawn from an extreme value distribution $\mathbf{EVT}(0, \sigma_{mn}^2)$. The values reported are the difference from the nominal level, expressed in percentage.

σ_{mn}	BNS	HT	AS - J ($\gamma = 4$)			FDA
			$k = 2$	$k = 3$	$k = 4$	
0	3.85	5.25	6.05	6.65	5.20	-0.20
	<u>Normal</u>					
0.027	-0.05	1.85	2.35	8.30	3.35	0.20
0.08	-0.65	0.85	12.45	-0.995	1.25	-0.05
	<u>EVT</u>					
0.027	0.75	6.05	15.50	19.55	13.05	0.10
0.08	-0.15	7.95	14.80	20.50	2.80	-0.10
	<u>Autocorrelated Noise</u>					
	1.70	2.35	0.70	8.35	-0.08	-0.25

Table 3: Sample statistics of the returns on exchange rates

	JPY/EUR	USD/EUR
Mean	0.0004	0.0110
Std.	1.0558	0.8420
Skew.	0.2728	-0.1469
Kurt.	29.5105	14.3109

Table 4: The difference (in percentage) of the ERR and the predetermined nominal levels of the return quantile of JPY/EUR. For AR(p) model: $p = 1 - 5, 7, 13$ for *RV*, $p = 1 - 5, 8, 13, 14$ for *BNS*, $p = 1 - 5, 13, 14$ for *HT*, and $p = 1 - 5, 7, 10, 15$ for *FDA*. For the Long-memory model: $p = 1, 3, 5$ for *RV*, $p = 1 - 3, 5, 6, 14$ for *BNS*, $p = 1 - 3, 5, 6, 14$ for *HT*, and $p = 1, 3, 15$ for *FDA*. We use the standard student distribution ($\xi = 1$), while $\nu = 15$ for *RV*, $\nu = 15$ for *HT*, $\nu = 12$ for *BNS*, and $\nu = \infty$ for *FDA*.

JPY/EUR				
<u>In-sample prediction</u>				
Variance measure	1%		99%	
	$N(0, 1)$	$st(\nu)$	$N(0, 1)$	$st(\nu)$
<i>RV</i>	0.52	0.07	-0.18	0.2
<i>BNS</i>	0.56	0.22	-0.33	0.09
<i>HT</i>	1.02	0.29	-0.52	0.12
<i>FDA</i>	0.22	0.22	-0.07	-0.07

<u>One-day ahead forecast</u>				
AR(p) model				
Variance measure	1%		99%	
	$N(0, 1)$	$st(\nu)$	$N(0, 1)$	$st(\nu)$
<i>RV</i>	0.68	0.29	-0.29	0.31
<i>BNS</i>	0.90	0.28	-0.29	0.09
<i>HT</i>	1.21	0.37	-0.37	0.01
<i>FDA</i>	0.45	0.45	-0.14	-0.14

Long-memory model				
Variance measure	1%		99%	
	$N(0, 1)$	$st(\nu)$	$N(0, 1)$	$st(\nu)$
<i>RV</i>	0.71	0.33	-0.09	0.38
<i>BNS</i>	0.95	0.27	-0.17	0.26
<i>HT</i>	1.10	0.4	-0.17	0.14
<i>FDA</i>	0.56	0.56	-0.06	0.56

Table 5: The difference (in percentage) of the ERR and the nominal levels of the return quantile of USD/EUR. For the AR(p) model: $p = 1 - 6, 11 - 13, 18, 19$ for *RV*, $p = 1 - 6, 11 - 13, 18$ for *BNS*, $p = 1 - 4, 5, 11 - 13, 18$ for *HT*, and $p = 1 - 5, 10, 13, 14$ for *FDA*. For the Long-memory model: $p = 1, 2, 4, 5, 6, 10, 18$ for *RV*, $p = 1 - 3, 5, 6, 13, 15, 18$ for *BNS*, $p = 1, 3, 4, 13, 15, 18$ for *HT*, and $p = 1, 5, 10, 14, 15$ for *FDA*. We use the standard student distribution ($\xi = 1$), while $\nu = 30$ for *RV*, $\nu = 20$ for *HT* and *BNS*, and $\nu = 57$ for *FDA*.

USD/EUR				
<u>In-sample prediction</u>				
Variance measure	1%		99%	
	$N(0, 1)$	$st(\nu)$	$N(0, 1)$	$st(\nu)$
<i>RV</i>	0.04	-0.16	-0.19	0.06
<i>BNS</i>	-0.19	-0.06	-0.36	0.03
<i>HT</i>	0.29	-0.08	-0.56	0.11
<i>FDA</i>	0.02	0.04	-0.12	0.11
<u>One-day ahead forecast</u>				
AR model				
Variance measure	1%		99%	
<i>RV</i>	1.08	0.64	-0.54	-0.33
<i>BNS</i>	1.08	0.74	-0.69	-0.44
<i>HT</i>	1.28	0.83	-0.98	-0.39
<i>FDA</i>	0.93	0.78	-0.54	-0.49
Long-memory model				
Variance measure	1%		99%	
<i>RV</i>	1.01	0.61	-0.56	-0.31
<i>BNS</i>	1.11	0.71	-0.61	-0.46
<i>HT</i>	1.32	0.76	-0.81	-0.46
<i>FDA</i>	1.06	0.81	-0.51	-0.46

Table 6: Expected Shortfall of JPY/EUR and USD/EUR Returns. The values reported are the difference from the expected value -2.6426 under the normal distribution.

	JPY/EUR	USD/EUR
<i>RV</i>	0.6754	0.2231
<i>BNS</i>	0.4644	0.1946
<i>HT</i>	0.5558	0.2805
<i>FDA</i>	0.0899	0.1541

Table 7: Out-of-sample forecast evaluation using Diebold and Mariano test as described in Sec 7.

	Full Sample	Rolling Sample
JPY/EUR		
<i>BNS</i>	1.9360	0.4448
<i>HT</i>	-1.9707	0.7547
<i>FDV</i>	-0.8548	-0.4947
USD/EUR		
<i>BNS</i>	-6.2287	-0.2898
<i>HT</i>	-2.902	0.8647
<i>FDV</i>	-7.1077	-1.8567

Table 8: ML estimation results for the \log realized variance with continuous volatility and jump components

	JPY/EUR		
	FDV	HT	BNS
Const.	.0018 (0.0348)	-0.0174 (0.0445)	-0.0003 (0.0356)
C_{t-1}	0.9155 (0.1024)	0.8488 (0.0942)	0.9526 (0.1093)
C_{t-5}	0.0638 (0.0705)	0.1149 (0.0641)	0.0371 (0.0744)
J_{t-1}	0.6033 (0.255)	0.416 (0.1034)	0.3096 (0.1929)
ϵ_{t-1}	-0.4506 (0.1205)	-0.3508 (0.1116)	-0.4944 (0.1265)
ϵ_{t-2}	-0.1578 (0.0824)	-0.0994 (0.0766)	-0.18 (0.0816)
ϵ_{t-6}	-0.1568 (0.0721)	-0.1512 (0.0718)	-0.1266 (0.0723)
	USD/EUR		
	FDV	HT	BNS
Const.	-0.037 (0.0526)	-0.0253 (0.0527)	-0.0259 (0.0529)
C_{t-1}	0.7899 (0.0906)	0.796 (0.0935)	0.821 (0.0915)
C_{t-5}	0.1563 (0.0518)	0.1484 (0.0531)	0.1364 (0.0513)
J_{t-1}	0.66 (0.2381)	0.2444 (0.0965)	0.2111 (0.16)
ϵ_{t-1}	-0.3808 (0.1035)	-0.3679 (0.0106)	-0.415 (0.1031)
ϵ_{t-2}	-0.0606 (0.0692)	-0.0687 (0.0715)	-0.0762 (0.0696)
ϵ_{t-6}	-0.1229 (0.0582)	-0.1229 (0.0586)	-0.1222 (0.058)

Table 9: GMM Estimation of the Volatility Forecasting Regression

Coef.	<i>FDV</i>	<i>RV</i>	<i>HT</i>	<i>BNS</i>
EUR/JPY				
α	0.7391 (0.8598)	-0.1519 (1.1142)	0.0542 (0.9929)	-0.0824 (1.1083)
β	1.1941 (0.0857)	1.2868 (0.1131)	1.1902 (0.1007)	1.2601 (0.1113)
R^2	0.7783	0.7387	0.7427	0.7299
χ^2 (p-value)	<.0.0001	< 0.0001	< 0.0001	< 0.0001
USD/EUR				
α	2.8383 (0.6708)	3.0145 (0.6798)	2.6167 (0.6509)	2.72 (0.6998)
β	0.8004 (0.0644)	0.8006 (0.0668)	0.7735 (0.0637)	0.7998 (0.069)
R^2	0.6827	0.6529	0.6616	0.6452
χ^2 (p-value)	< 0.0001	< 0.0001	< 0.0001	< 0.0001

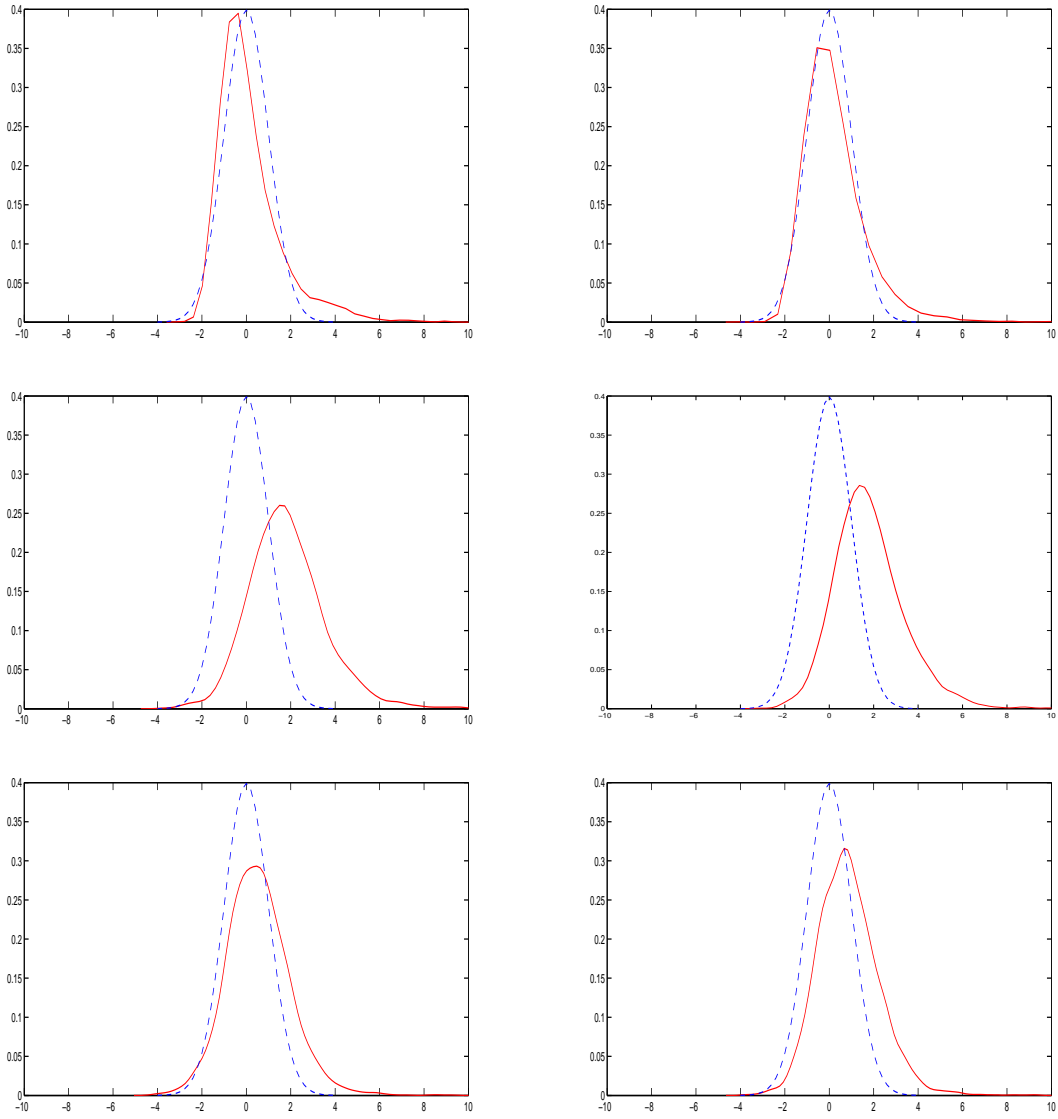


Figure 1: Density estimate of z_{TP} (solid curve) superimposed with standard normal density (dotted curve) for JPY/EUR and USD/EUR: The top panel uses the FDA method; the center panel uses the HT method; the bottom panel is based on the BNS bipower variation method.

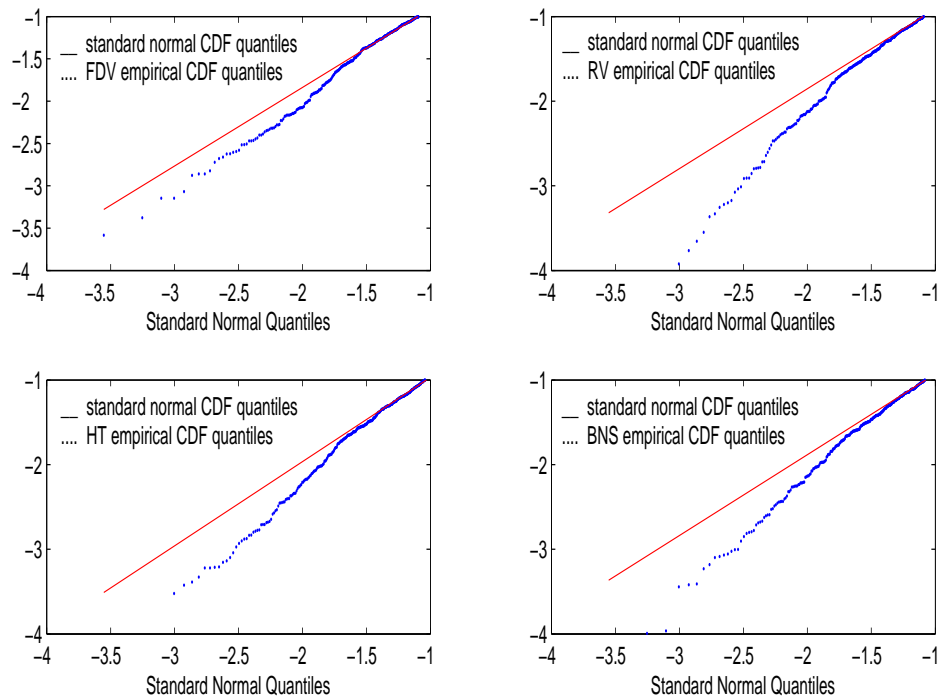


Figure 2: Quantile-quantile plots of standardized returns with standard normal density for JPY/EUR using various methods. Clockwise from left top: FDA, RV, Barndorff-Nielson and Shephard bipower variation (BNS) and staggered bipower variation (HT).

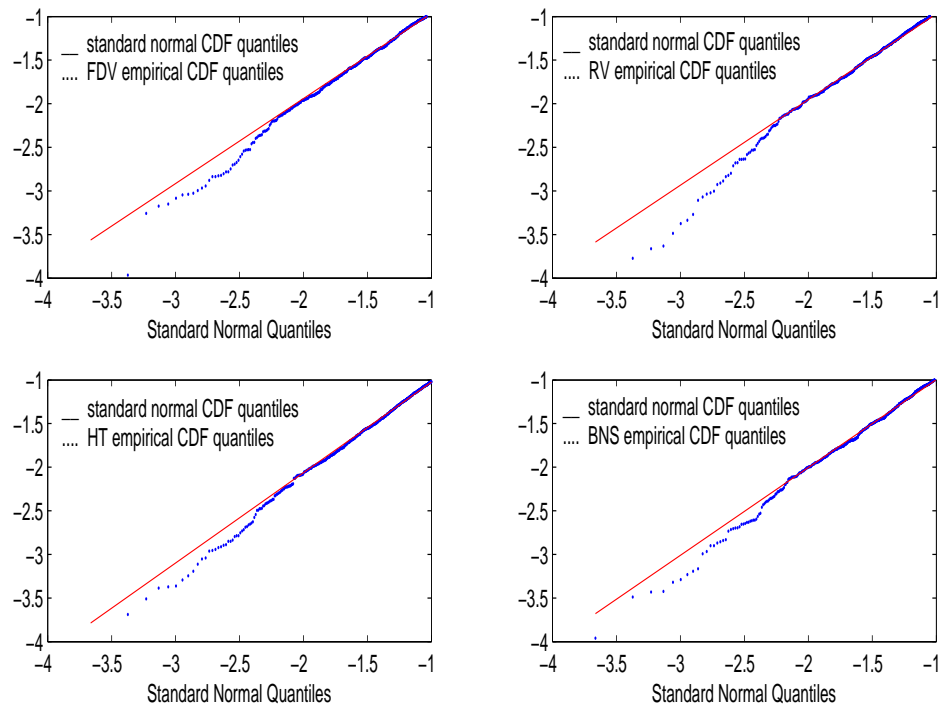


Figure 3: Quantile-quantile plots of standardized returns with standard normal density for USD/EUR using various methods. Clockwise from left top: FDA, RV, Barndorff-Nielson and Shephard bipower variation (BNS) and staggered bipower variation (HT).

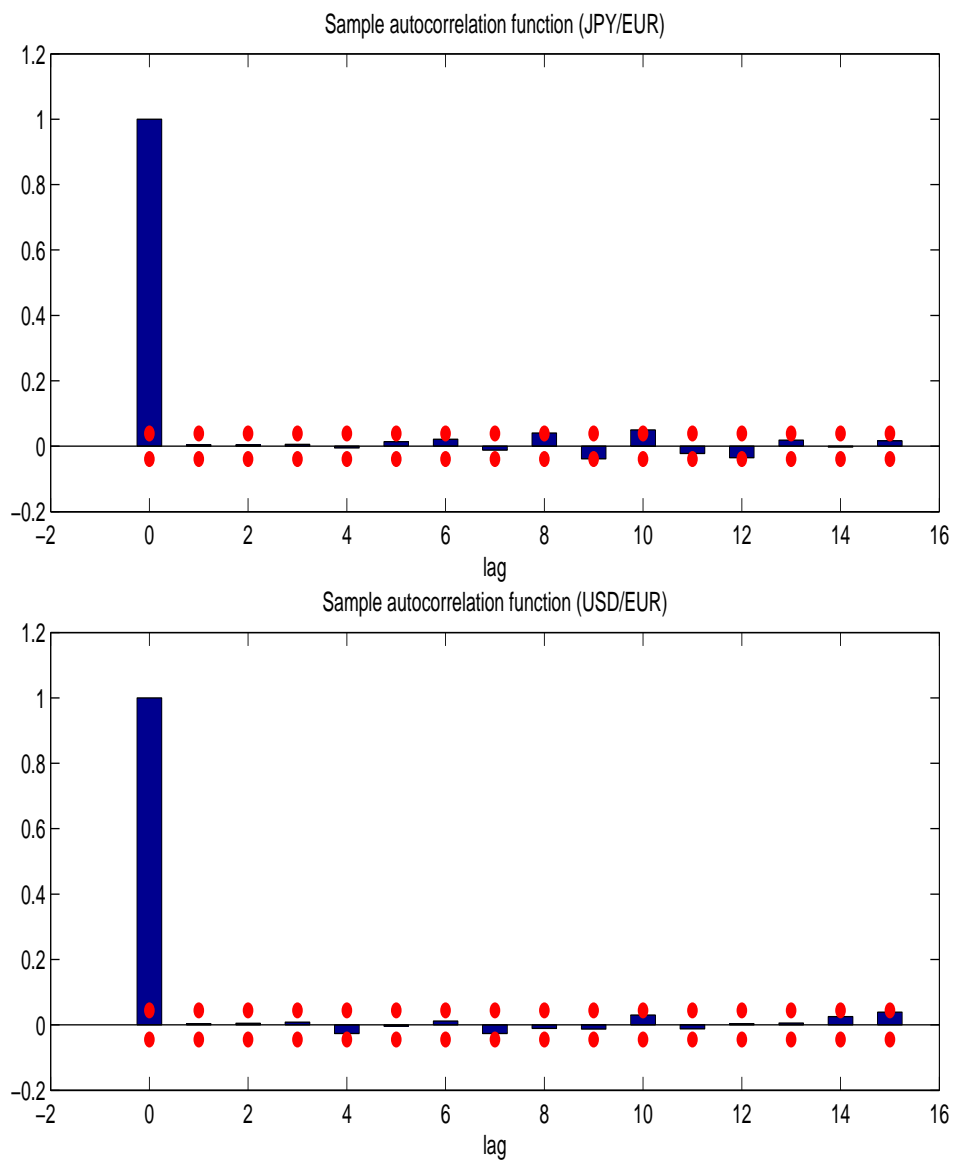


Figure 4: Sample autocorrelations of the residuals based on model (39). The dotted lines denote two standard-error limits of the sample autocorrelations.